Protein Science (1999), *8*:1350–1357. Cambridge University Press. Printed in the USA.

Formation of amyloid fibrils by peptides derived from the bacterial cold shock protein CspB

MICHAEL GROß,[1] DEBORAH K. WILKINS,[1] MAUREEN C. PITKEATHLY,[1]
EVONNE W. CHUNG,[1] CLAIRE HIGHAM,[2] ANNE CLARK,[2] AND CHRISTOPHER M. DOBSON[1]

[1]Oxford Centre for Molecular Sciences, University of Oxford, New Chemistry Laboratory, Oxford OX1 3QT, United Kingdom
[2]Department of Human Anatomy, University of Oxford, South Parks Road, Oxford OX1 3QT, United Kingdom

(RECEIVED January 8, 1999; ACCEPTED February 25, 1999)

Abstract

Three peptides covering the sequence regions corresponding to the first two (CspB-1), the first three (CspB-2), and the last two (CspB-3) β-strands of CspB, the major cold shock protein of *Bacillus subtilis*, have been synthesized and analyzed for their conformations in solution and for their precipitation behavior. The peptides are nearly insoluble in water, but highly soluble in aqueous solutions containing 50% acetonitrile (pH 4.0). Upon shifts of the solvent condition toward lower or higher acetonitrile concentrations, the peptides all form fibrils resembling those observed in amyloid associated diseases. These fibrils have been identified and characterized by electron microscopy, binding of the dye congo red, and X-ray fiber diffraction. Characterization of the peptides in solution by circular dichroism and NMR spectroscopy shows that the formation of these fibrils does not require specific preformed secondary structure in the solution state species. While the majority of the soluble fraction of each peptide is monomeric and unstructured, different types of structures including α-helical, β-sheet, and random coil conformations are observed under conditions that eventually lead to fibril formation. We conclude that the absence of tertiary contacts under solution conditions where binding interactions between peptide units are still favorable is a crucial requirement for amyloid formation. Thus, fragmentation of a sequence, like partial chemical denaturation or mutation, can enhance the capacity of specific protein sequences to form such fibrils.

Keywords: acetonitrile; aggregation; amyloid; β-sheet; circular dichroism; electron microscopy; misfolding; NMR spectroscopy

Proteins forming fibrillar aggregates have been shown to be associated with a wide range of medical conditions, including the prion diseases (Harrison et al., 1997), Alzheimer's disease (Beyreuther & Masters, 1997), familial amyloid polyneuropathy (Kelly, 1997), and type II diabetes (Westermark et al., 1987). Current structural models suggest that the main molecular features of these amyloid fibrils involve β-sheets organized as extended cross β structures with a helical twist (Blake & Serpell, 1996; Sunde & Blake, 1997), as a β-helix with between 9 and 24 residues per turn (Lazo & Downing, 1998), or as short, nontwisted β-sheets linked by loops (Jiménez et al., 1999). The mechanism of the formation of such proteinaceous fibrils is not known in molecular detail, although general models for specific cases have been proposed (Arvinte et al., 1993). The origin of amyloid deposit is also not well established. A sequence determinant, which makes a protein or peptide potentially amyloidogenic, has been proposed (Kurochkin, 1998), but the growing number of unrelated proteins forming fibrils closely similar to those found in amyloid deposits associated with chronical diseases suggests the propensity for this structure is inherent in the polypeptide backbone (Guijarro et al., 1998; Chiti et al., 1999). In this paper, all such fibrils will be called "amyloid fibrils" if they give the characteristic results in electron microscopy, congo red binding, and birefringence of congo red stained fibrils, whether or not they derive from pathogenic processes. A thorough understanding of the mechanisms and driving forces leading to amyloid fibril formation is required for the identification of novel strategies to prevent or cure the diseases with which they are associated.

In the context of a research project aimed at the folding of nascent protein chains (Groß, 1996; Groß & Dobson, 1997), we have investigated the solution properties of three synthetic pep-

Reprint requests to: Christopher M. Dobson, Oxford Centre for Molecular Sciences, University of Oxford, New Chemistry Laboratory, Oxford OX1 3QT, United Kingdom; e-mail: chris.dobson@chemistry.oxford.ac.uk.

Abbreviations: CD, circular dichroism; DQF-COSY, double-quantum filtered correlated spectroscopy; EM, electron microscopy; ESI-MS, electrospray mass spectrometry; FTIR, Fourier transform infrared spectroscopy; LM, light microscopy; NOE, nuclear Overhauser effect; NOESY, NOE spectroscopy; PTA, phosphotungstic acid; ROE, rotating frame Overhauser effect; ROESY, ROE spectroscopy; TFE, trifluoroethanol; TOCSY, total correlation spectroscopy; TPPI, time proportional phase incrementation.

tides derived from the cold shock protein CspB from *Bacillus subtilis.* CspB has been shown by X-ray crystallography (Schindelin et al., 1993) as well as by NMR (Schnuchel et al., 1993) to have a simple all β-sheet topology homologous to the S1 domain (Bycroft et al., 1997). Like S1 and the homologous *Escherichia coli* cold shock protein, CspA, the *Bacillus* protein has been shown to bind single-stranded RNA, and it is thought to act as an RNA chaperone in that it stops mRNA from forming unwanted secondary structure at low temperatures (Graumann & Marahiel, 1997; Graumann & Marahiel, 1998). CspB is remarkable for its ability to fold very rapidly (Schindler et al., 1995; Schindler & Schmid, 1996), and for its relatively low contact order (Plaxco et al., 1998) (i.e., a high proportion of contacts between residues close to each other in the linear sequence). As all the β-sheet forming interactions occur between strands that are neighboring in the sequence, secondary structure formation might be possible both during the synthesis on the ribosome and also within the short peptide fragments investigated here.

Although this protein is not related to any of the at least 18 known eukaryotic constituents of pathological amyloid fibrils (Sunde & Blake, 1997), we find that all three peptides in our study precipitate as fibrils with characteristics closely similar to mammalian amyloid from a variety of conditions where highly unstructured monomers are the prevailing species in solution. It follows that the initial secondary structure content of the monomeric polypeptide is not a major determinant of amyloid formation. The most important requirement appears to be the lack of ordered tertiary structure under conditions where interactions such as hydrogen bonds or hydrophobic contacts are still viable (Chiti et al., 1999). This requirement can be met either by conditions that induce at least partial unfolding of the intact protein, or by dissecting a polypeptide chain into shorter peptides that are unable to form cooperative globular structure, as we demonstrate in this paper. Here we present results that characterize both the fibrils and the solution state from which they arise.

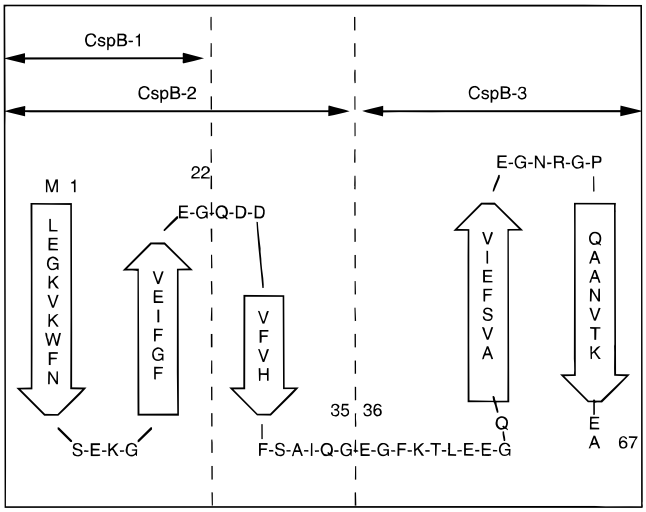

Fig. 1. Sequence and secondary structure content of the cold shock protein CspB from *Bacillus subtilis*. The numbers indicate the first and last amino acids of the three peptides used in this study: CspB-1 (1–22), CspB-2 (1–35), and CspB-3 (36–67).

Results and discussion

Based on the known structure of the *B. subtilis* cold shock protein CspB, consisting of five β-strands arranged in a small β sandwich (Schindelin et al., 1993; Schnuchel et al., 1993), the peptides CspB-1 (residues 1–22), CspB-2 (1–35), and CspB-3 (36–67) were designed to correspond to the first two, the first three, and the last two β-strands of the protein, respectively (Fig. 1). While CspB-1 and CspB-2 mimic a nascent protein growing from the N-terminus, CspB-2 and CspB-3 represent the two halves of the β sandwich and together cover the entire sequence length of the original protein.

Cold shock protein B is soluble in aqueous buffers at pH values ranging from 6.0 to 7.2 to a protein concentration of at least 1.3 mM (10 mg/mL), as demonstrated by the fact that the NMR structure was obtained under these conditions (Schnuchel et al., 1993). In contrast, neither of the three peptides investigated here is soluble under similar conditions to any significant extent; CspB-2, for example, dissolves only to ~0.2 mg/mL. To solubilize the peptides, we used acetonitrile as a cosolvent at pH 4.0 (formic acid, unbuffered). All three peptides are soluble to 10 mg/mL or higher under these conditions, although their solubility decreases drastically if the acetonitrile concentration is changed to values significantly higher or lower than 50%. For example, attempts to prepare NMR samples by diluting stock solutions containing 20 mg/mL peptide in 50% acetonitrile with four volumes of either water or acetonitrile resulted in rapid precipitation of the peptides. A standardized set of combinations of peptide concentration and solvent composition was used in the experiments described here, involving peptide concentrations of 0.4, 2, and 10 mg/mL, and acetonitrile concentrations of 10, 50, and 90%.

NMR studies of the three peptides were carried out under the conditions where they are most soluble (10 mg/mL peptide in 50% acetonitrile pH 4.0). CD studies were carried out at acetonitrile concentrations ranging from 5 to 95%. Due to the lower peptide concentrations needed for CD spectroscopy (0.4 mg/mL), spectra could still be obtained under conditions of relatively low solubility (i.e., in higher and lower concentrations of acetonitrile). The insoluble material produced by solvent shifts was analyzed by a variety of techniques including specific tests for the presence of amyloid fibrils.

CD measurements

The three peptides were found to differ substantially in their structural properties, as monitored by CD spectroscopy, particularly under the conditions where they are relatively insoluble and from which fibril formation can be initiated (see below). In the soluble state (50% acetonitrile), CspB-1 appears to be largely unstructured at 0.4 mg/mL (Fig. 2A,D), although it forms β-sheet structure at very high peptide concentrations, as indicated by additional CD measurements using a 0.1 mm pathlength cell. The ellipticity per residue increases from $-1{,}730$ to $-6{,}480$ deg cm^2/dmol as the acetonitrile concentration is increased to 90%, suggesting ~70% of β structure at the highest acetonitrile concentration.

CspB-2 (Fig. 2B,D) adopts a largely β-sheet conformation at very high and at very low acetonitrile concentrations (100% β-sheet at 2.5% acetonitrile, and 71.5% β-sheet at 97.5% acetonitrile). It is less structured at intermediate solvent conditions (mean residue ellipticities around $-3{,}410$ deg cm^2/dmol, indicating ~20% β-sheet content in the range from 15 to 70% acetonitrile). CspB-3

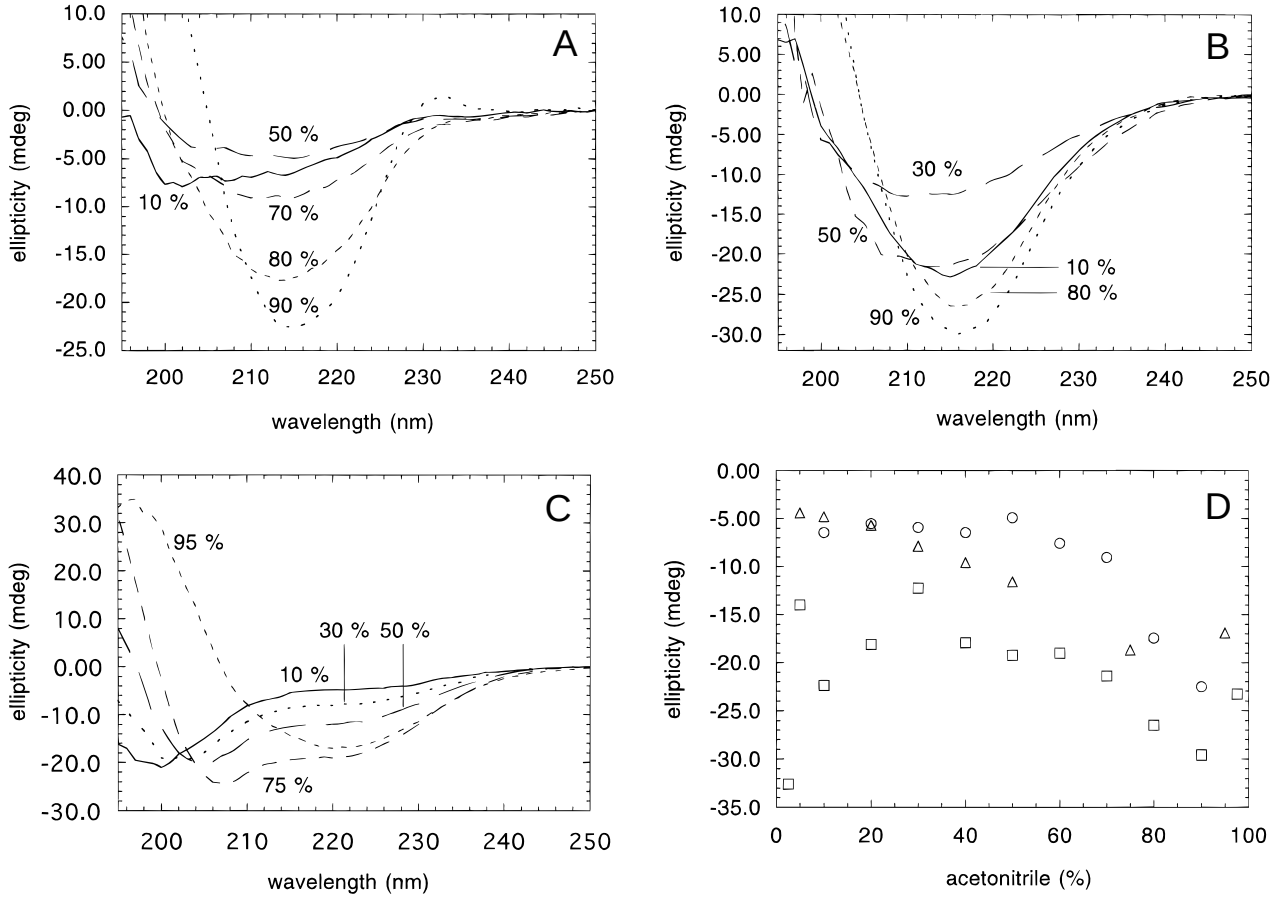

Fig. 2. Characterization of dilute solutions of the peptides by CD spectroscopy. Acetonitrile concentration was varied as indicated. **A–C:** CD spectra recorded at acetonitrile concentrations ranging from 2.5 to 97.5% of solutions containing 0.4 mg/mL of **(A)** CspB-1, **(B)** CspB-2, and **(C)** CspB-3. **D:** Ellipticity at 215 nm plotted against the acetonitrile concentration. Circles: CspB-1; squares: CspB-2, triangles: CspB-3.

(Fig. 2C,D) displays particularly interesting behavior as it can be in predominantly unstructured, partly helical, or largely β-sheet conformations depending on the acetonitrile concentration. The CD data show that the helix content increases gradually as the acetonitrile concentration is increased from 5 to 75%, but the peptide converts to predominant β-sheet structure at acetonitrile concentrations between 75 and 95%. At the latter concentration, the ellipticity per residue observed at 215 nM for this peptide is $-3{,}830$ deg cm^2/dmol, corresponding to 41% β-sheet.

At low concentrations of acetonitrile (10%), CspB-2 adopts a β-sheet conformation, while the other two peptides are predominantly unstructured. At high acetonitrile concentrations (90%), however, all peptides show some extent of β-sheet formation, which overlaps with random coil properties for the two N-terminal peptides, and with α-helical structure for the C-terminal peptide (Fig. 2). CspB-3 changes sequentially from unstructured to helical to β-sheet conformation when gradually transferred from 5 to 95% acetonitrile. Generally, therefore, the β-sheet content increases when the conditions change toward lower solubility or higher acetonitrile concentration. This is indicative of intermolecular rather than intramolecular β-sheet formation. The data suggest that the monomers are mostly unstructured (or partially helical in the case of CspB-3), while the aggregates all contain β structure.

NMR experiments

NMR diffusion measurements (Jones et al., 1997) conducted at a peptide concentration of 10 mg/mL in 50% acetonitrile indicate a single diffusion constant for each peptide, corresponding to values of hydrodynamic radii similar to those predicted for unfolded monomers (Table 1). This suggests that the samples consist predominantly of monomers. Any small oligomers (whose signals merge with the monomer signal if conformational interconversion takes place on a time scale shorter than that resolvable by this method, i.e., less than ~100 ms) can only exist as minor populations. Calibration of the spectral intensities, however, indicates that these are lower than expected for the concentration of peptide involved. This was examined quantitatively for CspB-1, where it was found that only ~20% of the total peptide concentration present in the sample is detectable in the NMR spectra. The remainder must therefore be in large soluble aggregates whose overall tumbling times are too large to give resolvable NMR resonances.

Detailed structural NMR studies of all three peptides were undertaken at 20 and at 35 °C in solutions containing 50% acetonitrile. For all peptides, complete assignment of the amide resonances was achieved by analysis of COSY and TOCSY spectra acquired

Table 1. *Hydrodynamic radii*[a] *of CspB peptides at 10 mg/mL concentration in 50% acetonitrile, as determined by NMR diffusion measurements*

Peptide (no. of residues)	Hydrodynamic (Stokes) radius (nm)[b]	Predicted value for unfolded monomer (nm)[c]	Predicted value for unfolded dimer (nm)
CspB-1 (22)	1.60[a]	1.29	1.80
CspB-2 (35)	1.68	1.72	2.54
CspB-3 (32)	1.66	1.63	2.43

[a] Hydrodynamic radii were calculated using Stokes' law from diffusion measurements as described previously (Jones et al., 1997). The Stokes radius of CspB-1 was also determined in the supernatant of a sample containing 2 mg/mL peptide in 10% acetonitrile after fibril formation was completed. The Stokes radius of this species was 1.34 nm.

[b] HPLC analysis confirms that the peptides in their soluble states are largely monomeric, but provides evidence for minor populations of small oligomers. In chromatographic profiles, monomers are the dominant species, while dimers and higher order oligomers are present only at lower concentrations (<30%).

[c] Predictions are based on a fit of the hydrodynamic radii measured by pulse field gradient NMR for highly unfolded proteins and peptides, resulting in the empirical equation $R = 0.225N^{0.57}$ where R is the hydrodynamic radius in nm and N is the number of amino acid residues (D.K. Wilkins, J.A. Jones, V. Receveur, S.B. Grimshaw, L.J. Smith, C.M. Dobson, unpubl. results).

at 35 °C. None of the peptides showed any measurable long range NOEs or ROEs. This indicates the absence of any significant persistent structure. The structural characteristics of the peptides were therefore inferred by comparing their chemical shifts and coupling constants with those predicted from random coil models (Serrano, 1995; Smith et al., 1996). Although random coil values of chemical shifts are well documented (Wishart et al., 1995; Plaxco et al., 1997), the values obtained for amide protons are highly dependent on solvent conditions. Therefore, we used only the C_α proton shifts in this analysis. These show only minor deviations from typical random coil values (most between ± 0.1, and all between -0.20 and $+0.15$ ppm).

Most of the coupling constants measured for CspB-1 are slightly larger than the values predicted for a random coil (Smith et al., 1996) (Fig. 3A). This indicates that CspB-1 has a slightly higher occupancy of the β-region of $\phi\psi$ space than anticipated for a random coil. This is most pronounced in the regions of residues 5–9 and 17–20 (Fig. 3A). Both these groups of residues are within the regions of the β-strands in the native protein (2–10, 15–20). For CspB-3, the coupling constant measurements show smaller values than predicted for a random coil, suggesting that the small amount of helical structure observed in the CD spectra is likely to be localized between residues 38 and 53 (Fig. 3B). This result is also in accord with the slight propensity for helix formation in this region revealed by several of the secondary structure prediction methods used. Thus, the Gibrat (Gibrat et al., 1987), Levin (Levin et al., 1986), DPM (Deleage & Roux, 1987), and SOPMA (Geourjon & Deleage, 1995) methods predict the conformation of the majority of the residues in positions 38 to 47 to be helical (data not shown). Additional helicity, which is predicted to occur near the carboxy terminus, was not observed by NMR.

Evidence for amyloid fibril formation

Analysis by three independent techniques of samples produced by dilution of concentrated solutions of all three peptides (10.0 mg/mL diluted to 2.0 mg/mL final concentration) from 50% to either 10 or 90% acetonitrile was carried out to screen for the presence of amyloid fibrils. CspB-1 was used for all further investigations into fibril formation. Spectroscopic binding assays using the diazo dye congo red (Fig. 4A) show the typical red shift in wavelength and increase in intensity characteristic of amyloid fibrils. In transmission electron microscopy (Fig. 4B), a dense network of straight and unbranched fibrils approximately 10 nm in diameter and up to 300 nm long was observed for CspB-1 diluted into 10% acetonitrile. Under other experimental conditions, and with the other peptides, fewer fibrils were observed, but similar morphologies were evident. Light microscopy of congo red stained precipitates using crossed polarizers (not shown) revealed the green birefringence characteristic of amyloid fibrils (Cooper, 1974).

Aggregated states of all three peptides produced in 10 and 90% acetonitrile were analyzed using these techniques. While all types of experiment were strongly positive for the presence of amyloid for CspB-1 in 10% acetonitrile, more varied results were obtained under some of the other conditions. Nevertheless, under all conditions positive evidence indicating formation of amyloid fibrils was obtained (Table 2).

Further examination was carried out with the fibrils formed by CspB-1 in 10% acetonitrile. Intermolecular β-sheet structure, which is compatible with fibril formation, was also demonstrated by FTIR (D.K. Wilkins, M. Groß, & C.M. Dobson, unpubl. results) for peptide CspB-1. X-ray fiber diffraction also yielded results characteristic of amyloid fibrils. For the latter technique, a sample of CspB-1 in 50% acetonitrile was left to dry down after suspending between two capillaries. As a result of the higher volatility of acetonitrile, the solvent composition changes during the evaporation and is expected to be near 10% acetonitrile during the actual precipitation process. This resulted in a thin needle of precipitate, which showed X-ray diffraction patterns (Fig. 4C,D) with diffraction maxima at 0.47 and 1.04 nm, typical of amyloid fibrils (Sunde & Blake, 1997).

Conclusions

We have shown that three peptides derived from a small bacterial protein with an all β structure can form amyloid fibrils, although there is no known link to a pathogenic amyloid forming protein. The formation of these fibrils can occur from quite different starting situations by solvent shifts toward higher or lower concentrations of acetonitrile. Typically, the solutions contain populations of largely unstructured monomers, together with oligomers and soluble aggregates containing significant amounts of β-sheet structure. This suggests that amyloid formation does not depend on the presence of extensive preformed secondary structure elements within monomeric species in solution, although the aggregates and the amyloid fibrils themselves contain extensive β-sheet structure. More generally, β structure is common within a wide range of aggregates of different morphologies (Fink, 1998). The ability to form aggregates with such β structure is likely to be an important factor in the subsequent conversion to ordered amyloid fibrils.

As far as the primary structure is concerned, a sequence motif, which is recognized by the insulin degrading enzyme (IDE), has recently been suggested to be a determinant for the formation of amyloid fibrils (Kurochkin, 1998). However, no such motif is

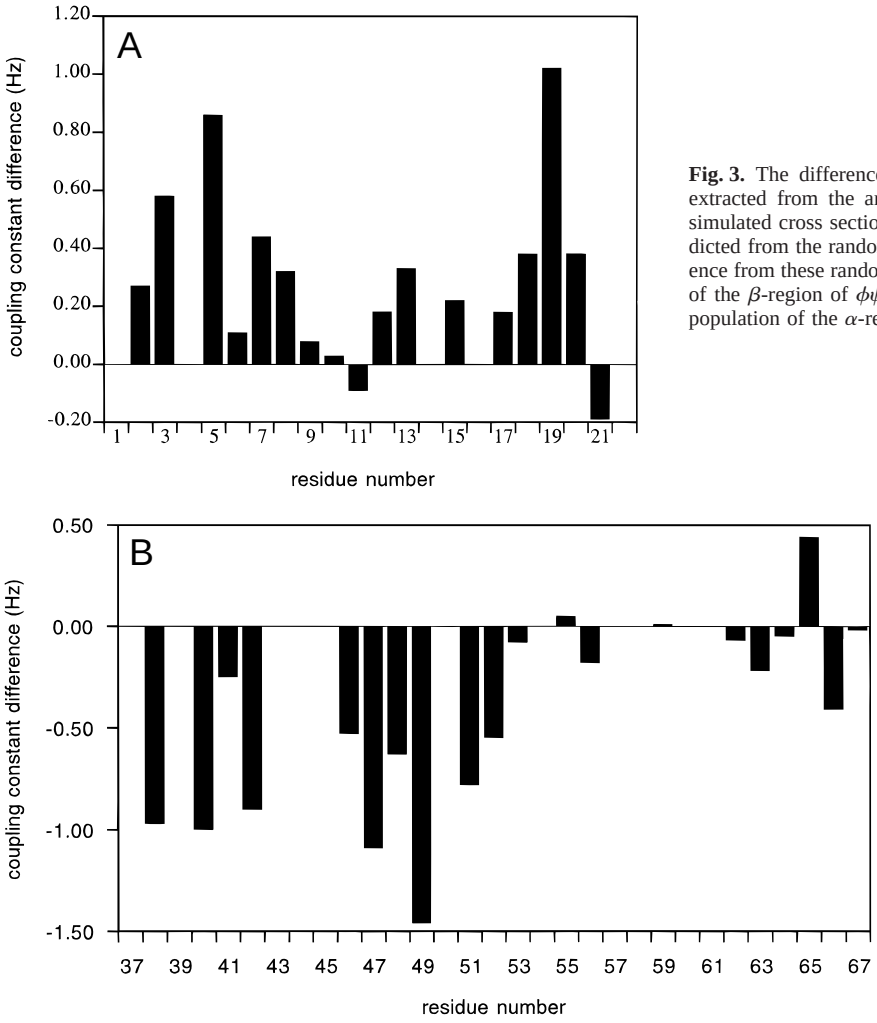

Fig. 3. The difference of the residue specific $^3J_{NH\alpha}$ coupling constants extracted from the antiphase splitting in a COSY spectra by fitting to simulated cross sections for **(A)** CspB-1 and **(B)** CspB-3 from those predicted from the random coil model (Smith et al., 1996). A positive difference from these random coil values indicates an increase in the population of the β-region of $\phi\psi$ space, and negative differences an increase in the population of the α-region.

present in any of the three peptides studied here. Similarly, the SH3 domain from bovine phosphatidyl inositol 3-kinase, an 84 residue protein with five β-strands, which readily forms amyloid fibrils at acidic pH (Guijarro et al., 1998), does not contain such a motif. One protofilament structure proposed recently (Lazo & Downing, 1998) requires short β-strands with hydrophobic residues in every other position. Such sequence elements are indeed found in all of the CspB peptides studied here (e.g., residues 5–9, 47–51 in CspB, see Fig. 1), and in the sequence of the PI3–SH3 domain (e.g., residues 23–29: DIDLHLG). While the sequences matching this criterion provide some support for such a structural model, this sequence motif is not specific enough to draw strong conclusions from it.

It has been suggested that the formation of the characteristic cross β structure of the amyloid fibrils, in which the β-strands are oriented perpendicular to the fiber axis, reflects a natural bias of the polypeptide chain (Sunde & Blake, 1997). That this is not normally observed in biological systems is likely to arise predominantly from the cooperative formation of specific tertiary interactions characteristic of native globular proteins (Chiti et al., 1999). In denaturing conditions and in short peptides, therefore, the absence of specific tertiary interactions allows intermolecular interactions, which can ultimately lead to the formation of fibrillar structures.

The tertiary structure of a protein can be destabilized by partial denaturation, by mutation, or by dissection into short fragments. For example, the SH3 domain was shown to form amyloid fibrils from a partially folded low pH state (Guijarro et al., 1998), a fibronectin module behaves similarly when heated (Litvinovich et al., 1998), as does acylphosphatase when it is dissolved in trifluoroethanol (TFE) at concentrations just sufficient to denature the protein (Chiti et al., 1999). In human lysozyme, a single destabilizing point mutation is sufficient to turn a normally stable monomeric protein into an amyloidogenic variant (Pepys et al., 1993; Booth et al., 1997). Moreover, short peptides derived from the amyloidogenic proteins transthyretin (Serpell, 1995), prions (Pillot et al., 1997), or Alzheimer-associated proteins (Han et al., 1995) can have stronger propensities to form amyloid fibrils than the full length proteins.

Here we have demonstrated therefore that peptides derived from a soluble globular protein not related to any pathogenic sequences can form amyloid fibrils. This reinforces the view that amyloid formation is a generic property of polypeptide chains, and that destabilization of tertiary structure is a major requirement for the formation of such aggregates. The latter suggests that agents enhancing the tertiary structure without increasing the secondary structure propensities of proteins could be useful as inhibitors of the pathological process of amyloidosis (Peterson et al., 1998). On the other hand, agents that favor secondary over tertiary structure may promote the growth of amyloid fibrils, as demonstrated by the

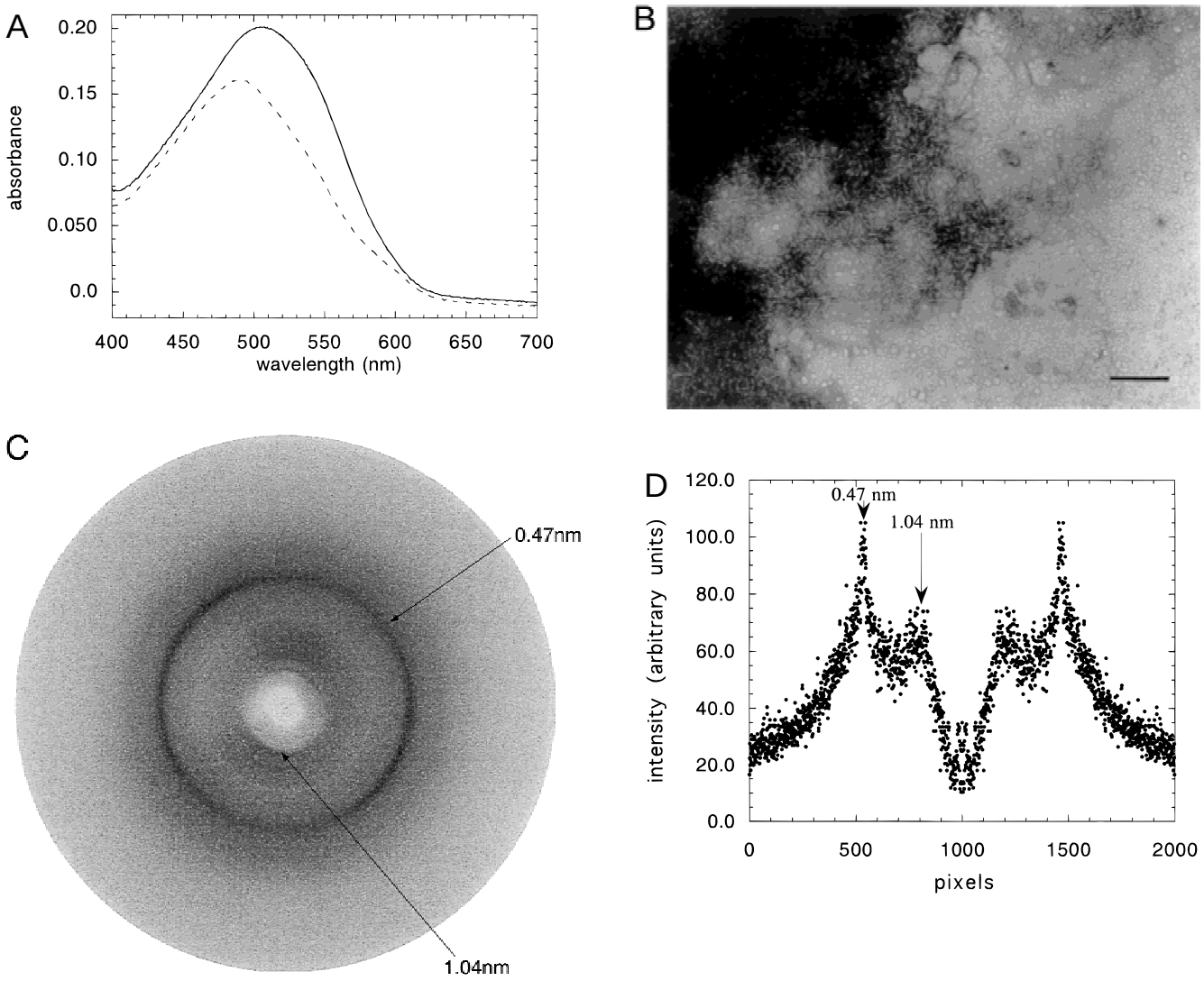

Fig. 4. Evidence for amyloid fibrils formed by CspB-1 upon reduction of the acetonitrile concentration. **A:** Example of the visible spectra of the congo red assay. The dashed line represents the spectrum before, the solid line the one after, addition of a sample of CspB-1 in 10% acetonitrile. The shift toward higher wavelengths and greater intensity indicates fibril formation. **B:** Electron micrograph of negatively stained fibrils. The scale bar corresponds to a length of 200 nm. **C:** X-ray fiber diffraction pattern obtained from a sample dried down from a 5 mg/mL solution in 50% acetonitrile. **D:** Cross section of the diffraction pattern in **C** with assignment of the peaks corresponding to the distances typical for β-sheet structure.

effect of TFE on acylphosphatase (Chiti et al., 1999). It is difficult to determine the localized conditions that affect misfolding events at the site of amyloid formation in vivo. Understanding the molecular details of the events giving rise to amyloid formation is, however, an important step in the quest to develop diagnostic and therapeutic agents for amyloid-related diseases. Given that amyloid fibril formation can be easily triggered in the peptides reported here, they present a suitable model for kinetic and mechanistic studies of fibril formation.

Materials and methods

Peptide synthesis

Peptides were assembled on an Applied Biosystems (Foster City, California) 430A automated peptide synthesizer using the base-labile 9-fluorenylmethoxycarbonyl (Fmoc) group for the protection of the α-amino function. Side-chain functionalities were protected by the t-Bu (Asp, Ser, Thr, Tyr), trityl (Asn, Gln), or the Pmc (Arg) group. Synthesis and purification were carried out as described previously (Yang et al., 1994). The identity and purity of the peptides were confirmed by ESI-MS. The masses measured for CspB-1, CspB-2, and CspB-3 were 2,531.1, 3,976.6, and 3,449.5 g/mol, respectively (masses predicted from the sequence: 2,531.9, 3,976.6, 3,448.7).

Sample preparation

All three peptides were found to have optimal solubility if first dissolved in 50% acetonitrile pH 4.0 (adjusted with formic acid, unbuffered), and subsequently diluted to the desired peptide and acetonitrile concentrations.

Table 2. *Overview of results obtained in a series of two screening experiments to assess the formation of amyloid fibrils under different conditions, using congo red binding, EM, and detection of the green birefringence by light microscopy (LM)*[a]

Condition	Method	CspB-1	CspB-2	CspB-3
10% acetonitrile	Congo red	++, ++	++, o	++, ++
	EM	++	++	+
	LM	++, ++	+	++, +
90% acetonitrile	Congo red	++, o	o, ++	++, +
	EM	o	++	o
	LM	++, ++	++, o	o, ++

[a]The final peptide concentration was 1.6 mg/mL for the first congo red experiment carried out under each set of conditions and 2.0 mg/mL for all other experiments. Results: (++) strongly positive, (+) weakly positive, (o) no positive evidence. In addition to the results shown here, fibril formation in 10% acetonitrile was observed in many more experiments carried out with CspB-1 in separate studies (D.K. Wilkins, M. Groß, I. Schofield, & C.M. Dobson, unpubl. results).

Optical spectroscopy

CD spectra were recorded on a Jasco J720 spectropolarimeter using quartz cuvettes of 1 mm pathlength, at 1 nm intervals from 195 to 250 nm. Routinely, CD samples were examined 30 min after dilution from the peptide stock solution containing 50% acetonitrile. Kinetic experiments revealed that, after this time, given the relatively low concentration (0.4 mg/mL) of the CD samples, no time dependent effects could be observed on the timescale of minutes.

Calculation of the β-sheet content was carried out using the ellipticity at 215 nm normalized to a per residue basis (units: deg cm^2/dmol). The highest value observed in this study ($-$9,260 deg cm^2/dmol) was taken to correspond to 100% β structure, which agrees well with the value proposed by other workers ($-$9,210 deg cm^2/dmol at 216 nm (Chen et al., 1974)).

For the congo red binding assay of fibril formation, absorption spectra of a 10 μM solution of the dye in the assay buffer (5 mM phosphate pH 7.4, 0.15 mM NaCl) before and after addition of the peptide solution were recorded on a Perkin Elmer (Foster City, California) Lambda 16 spectrometer in the range of 400 to 700 nm. Typically, 10 μL of the peptide sample were used in a total volume of 1.0 mL.

NMR spectroscopy

All NMR spectra were acquired at ^{1}H frequencies of 500 or 600 MHz on homebuilt NMR spectrometers at the Oxford Centre for Molecular Sciences. One-dimensional (1D) spectra typically contain 8K complex data points. Two-dimensional (2D) experiments were acquired with 2K complex data points in the t_2 dimension, and in phase-sensitive mode using time proportional phase incrementation (TPPI) (Marion & Wüthrich, 1983) for quadrature detection in t_1. Diffusion constants were determined using pulse field gradient experiments (Jones et al., 1997) with 8K complex points. Spectral widths of 8,000 Hz were used for all experiments. For the resonance assignments, DQF-COSY, TOCSY, ROESY, and NOESY spectra were recorded, involving between 512 and 800 t_1 increments with 32 to 128 scans each. The water signal was suppressed either by using presaturation during the 1.2 s relaxation delay or by using a gradient double echo (Schleucher et al., 1994). The mixing times for the TOCSY experiments varied between 23 and 60 ms, and for the NOESY and ROESY experiments between 100 and 260 ms. Data were processed using Felix 2.3 (BIOSYM) on Sun workstations. Typically, the data were zero filled once, and processed with a double exponential window function for the 1D, and a sinebell squared function shifted over 90° for each dimension of the 2D spectra. All spectra were referenced to an internal standard of dioxan at 3.743 ppm.

For the determination of the $^3J_{HN\alpha}$ coupling constants, high resolution DQF-COSY spectra were recorded with 4K complex points zero filled to 8K, and the window functions GM 3.75 and TM 16 4096 4096 applied. The cross peaks were then fitted to simulated antiphase cross sections along the F2 dimension using a procedure implemented in the Felix 2.3 program.

A series of 1D spectra was used to estimate the percentage of peptide visible by solution NMR. These 1D spectra were all acquired with 256 scans on the same 500 MHz NMR spectrometer, in consecutive experiments. The concentration of a tryptophan solution was calculated from its absorbance at 280 nm. The integration of the indole resonances in these 1D spectra from the tryptophan and peptide solutions was used to estimate the concentration of the peptide solutions.

Electron microscopy

Fibril formation and morphology were examined by transmission electron microscopy (EM). Peptide samples were dried onto formvar- and carbon-coated grids and negatively stained with 1% phosphotungstic acid (PTA). Grids were examined in a JEOL JEM-1010 electron microscope at 80 kV excitation voltage.

Light microscopy

Confirmation of the presence of amyloid fibrils in peptide samples was obtained by drying congo red stained fibrils onto glass slides and examining the preparations through a binocular microscope using crossed polarizers. Yellow green birefringence indicates the presence of cross β structure (Cooper, 1974).

X-ray fiber diffraction

Droplets of 10 μL peptide solution were suspended between the ends of two capillaries sealed with wax. While the normal procedure involves evaporation of the solvent over a timescale of $\sim$1 day, the presence of acetonitrile in the samples allowed the droplet to evaporate in approximately 1 h. Diffraction patterns of the remaining solid in the form of two thin needles attached to the ends of the capillaries were collected using a Cu K_α rotating anode equipped with a 180 mm image plate (MAR Research, Hamburg, Germany). The diffraction pattern was analyzed using the MarView software (MAR Research).

Supplementary material in Electronic Appendix

Resonance assignments for all three peptides are provided. Table 1 contains chemical shifts and coupling constants for CspB-1. Table 2 contains chemical shifts for CspB-2. Table 3 contains chemical shifts and coupling constants for CspB-3.

Acknowledgments

The Oxford Centre for Molecular Sciences is funded by the U.K. Biotechnology and Biological Sciences, Engineering and Physical Sciences, and Medical Research Councils (BBSRC, EPSRC, and MRC). M.G. is a David Phillips research fellow of the BBSRC. We are grateful to the British Diabetic Association (C.H.) and the Wellcome Trust (A.C., C.M.D.) for financial support. The research of C.M.D. is funded in part by an International Research Scholars award from the Howard Hughes Medical Institute and by the Wellcome Trust. The JEOL electron microscope was purchased by a grant from the Wellcome Trust. Help and advice from Mark Bartlam, Peter Graumann, Karl Harlos, Emma Jaikaran, Mohamed Marahiel, Chris Ponting, Carol Robinson, Shama Shah, Lorna Smith, and Margaret Sunde are gratefully acknowledged.

References

Arvinte T, Cudd A, Drake AF. 1993. The structure and mechanism of formation of human calcitonin fibrils. *J Biol Chem 268*:6415–6422.

Beyreuther K, Masters CL. 1997. Alzheimer's disease: The ins and outs of amyloid-β. *Nature 389*:677–678.

Blake C, Serpell L. 1996. Synchrotron X-ray studies suggest that the core of the transthyretin amyloid fibril is a continuous β-sheet helix. *Structure 4*:989–998.

Booth DR, Sunde M, Bellotti V, Robinson CV, Hutchinson WL, Fraser PE, Hawkins PN, Dobson CM, Radford SE, Blake CCF, Pepys MB. 1997. Instability, unfolding, and aggregation of human lysozyme variants underlying amyloid fibrillogenesis. *Nature 385*:787–793.

Bycroft M, Hubbard TJP, Proctor M, Freund SMV, Murzin AG. 1997. The solution structure of the S1 RNA binding domain: A member of an ancient nucleic acid-binding fold. *Cell 88*:235–242.

Chen Y-H, Yang JT, Chau KH. 1974. Determination of the helix and beta form of proteins in aqueous solution by circular dichroism. *Biochemistry 13*:3350–3359.

Chiti F, Webster P, Taddei N, Stefani M, Ramponi G, Dobson CM. 1999. Designing conditions for in vitro formation of amyloid fibrils. *Proc Natl Acad Sci USA 96*:3590–3594.

Cooper JH. 1974. Selective amyloid staining as a function of amyloid composition and structure. *Lab Invest 31*:232–238.

Deleage G, Roux B. 1987. An algorithm for protein secondary structure prediction based on class prediction. *Protein Eng 1*:289–294.

Fink AL. 1998. Protein aggregation: Folding aggregates, inclusion bodies and amyloid. *Folding Design 3*:R9–R23.

Geourjon C, Deleage G. 1995. Significant improvements in protein secondary structure prediction by prediction from multiple alignments. *Comput Appl Biosci 11*:681–684.

Gibrat JF, Garnier J, Robson B. 1987. Further developments of protein secondary structure prediction using information-theory—New parameters and consideration of residue pairs. *J Mol Biol 198*:425–443.

Graumann P, Marahiel MA. 1997. Effects of heterologous expression of CspB, the major cold shock protein of *Bacillus subtilis*, on protein synthesis in *Escherichia coli*. *Mol Gen Genet 253*:745–752.

Graumann PL, Marahiel MA. 1998. A superfamily of proteins that contain the cold-shock domain. *Trends Biochem Sci 23*:286–290.

Groß M. 1996. Linguistic analysis of protein folding. *FEBS Lett 390*:249–252.

Groß M, Dobson CM. 1997. Folding of nascent protein chains. *Chimia 51*:443.

Guijarro JI, Sunde M, Jones JA, Campbell ID, Dobson CM. 1998. Amyloid fibril formation by an SH3 domain. *Proc Natl Acad Sci USA 95*:4224–4228.

Han H, Weinreb PH, Lansbury PT. 1995. The core Alzheimer's peptide NAC forms amyloid fibrils which seed and are seeded by β-amyloid: Is NAC a common trigger of target in neurodegenerative disease? *Chem Biol 2*:163–169.

Harrison PM, Bamborough P, Daggett V, Prusiner SB, Cohen FE. 1997. The prion folding problem. *Curr Op Struct Biol 7*:53–59.

Jiménez JL, Guijarro JI, Orlova E, Zurdo J, Dobson CM, Sunde M, Saibil HR. 1999. Cryo-electron microscopy structure of an SH3 amyloid fibril and model of the molecular packing. *EMBO J 18*:815–821.

Jones JA, Wilkins DK, Smith LJ, Dobson CM. 1997. Characterization of protein unfolding by NMR diffusion measurements. *J Biomol NMR 10*:199–203.

Kelly JW. 1997. Amyloid fibril formation and protein misassembly: A structural quest for insights into amyloid and prion diseases. *Structure 5*:595–600.

Kurochkin IV. 1998. Amyloidogenic determinant as a substrate recognition motif of insulin-degrading enzyme. *FEBS Lett 427*:153–156.

Lazo ND, Downing DT. 1998. Amyloid fibrils may be assembled from β-helical protofibrils. *Biochemistry 37*:1731–1735.

Levin JM, Robson B, Garnier J. 1986. An algorithm for secondary structure determination in proteins based on sequence similarity. *FEBS Lett 205*:303–308.

Litvinovich SV, Brew SA, Aota S, Akiyama SK, Haudenschild C, Ingham KC. 1998. Formation of amyloid-like fibrils by self-association of a partially unfolded fibronectin type III module. *J Mol Biol 280*:245–258.

Marion D, Wüthrich K. 1983. Application of phase-sensitive two-dimensional correlated spectroscopy (COSY) for measurements of H1-H1 spin-spin coupling constants in proteins. *Biochem Biophys Res Comm 113*:967–974.

Pepys MB, Hawkins PN, Booth DR, Vigushin DN, Tennent GA, Soutar AK, Totty N, Nguyen O, Blake CCF, Terry CJ, Feest TG, Zalin AM, Hsuan JJ. 1993. Human lysozyme gene mutations cause hereditary systemic amyloidosis. *Nature 362*:553–556.

Peterson S, Klabunde T, Lashuel H, Purkey H, Sacchettini J, Kelly J. 1998. Inhibiting transthyretin conformational changes that lead to amyloid fibril formation. *Proc Natl Acad Sci USA 95*:12956–12960.

Pillot T, Lins L, Goethals M, Vanloo B, Baert J, Vandekerckhove J, Rosseneu M, Brasseur R. 1997. The 118–135 peptide of the human prion protein forms amyloid fibrils and induces liposome fusion. *J Mol Biol 274*:381–393.

Plaxco KW, Morton CJ, Grimshaw SB, Jones JA, Pitkeathly MC, Campbell ID, Dobson CM. 1997. The effects of guanidine hydrochloride on the random coil conformations and NMR chemical shifts of the peptide series GGXGG. *J Biomol NMR 10*:221–230.

Plaxco KW, Simons KT, Baker D. 1998. Contact order, transition state placement and the refolding rates of single domain proteins. *J Mol Biol 277*:985–994.

Schindelin H, Marahiel MA, Heinemann U. 1993. Universal nucleic acid binding domain revealed by crystal structure of the *Bacillus subtilis* major cold-shock protein. *Nature 364*:164–168.

Schindler T, Herrler M, Marahiel MA, Schmid FX. 1995. Extremely rapid protein folding in the absence of intermediates. *Nature Struct Biol 2*:663–673.

Schindler T, Schmid FX. 1996. Thermodynamic properties of an extremely rapid protein folding reaction. *Biochemistry 35*:16833–16842.

Schleucher J, Schwendinger M, Sattler M, Schmidt P, Schedletzky O, Glaser SJ, Sorensen OW, Griesinger C. 1994. A general enhancement scheme in heteronuclear multidimensional NMR employing pulsed-field gradients. *J Biomol NMR 4*:301–306.

Schnuchel A, Wiltscheck R, Czisch M, Herrler M, Willimsky G, Graumann P, Marahiel MA, Holak TA. 1993. Structure in solution of the major cold-shock protein from *Bacillus subtilis*. *Nature 364*:169–171.

Serpell LC. 1995. Structural studies of amyloid proteins. University of Oxford.

Serrano L. 1995. Comparison between the phi distribution of the amino acids in the protein database and NMR data indicates that amino acids have various phi propensities in the random coil conformation. *J Mol Biol 254*:322–333.

Smith LJ, Fiebig KM, Schwalbe H, Dobson CM. 1996. The concept of a random coil: Residual structure in peptides and denatured proteins. *Folding Design 1*:R95–R106.

Sunde M, Blake C. 1997. The structure of amyloid fibrils by electron microscopy and X-ray diffraction. *Adv Prot Chem 50*:123–159.

Westermark P, Wernstedt C, Wilander E, Hayden DW, O'Brien TD, Johnson KH. 1987. Amyloid fibrils in human insulinoma and islets of Langerhans of the diabetic cat are derived from a neuropeptide-like protein also present in normal islet cells. *Proc Natl Acad Sci USA 84*:3881–3885.

Wishart DS, Bigam CG, Holm A, Hodges RS, Sykes BD. 1995. ^{1}H, ^{13}C and ^{15}N random coil NMR chemical shifts of the common amino acids. I. Investigations of nearest-neighbor effects. *J Biomol NMR* 5:67–81.

Yang JJ, Pitkeathly M, Radford SE. 1994. Far-UV circular dichroism reveals a conformational switch in a peptide fragment from the β sheet of hen lysozyme. *Biochemistry 33*:7345–7353.